Geomechanics and Engineering, *Vol. 10, No. 4 (2016) 455-470*
DOI: http://dx.doi.org/10.12989/gae.2016.10.4.455

Importance of particle shape on stress-strain behaviour of crushed stone-sand mixtures

Janaka J. Kumara [*1] and Kimitoshi Hayano [2a]

[1] *Department of Civil Engineering, Tokyo University of Science, 2641, Yamazaki, Noda, Chiba 278-8510, Japan*
[2] *Department of Urban Innovation, Yokohama National University, 79-5, Tokiwadai, Hodogaya-ku, Yokohama, Kanagawa 240-8501, Japan*

(*Received December 09, 2014, Revised July 01, 2015, Accepted January 12, 2016*)

Abstract. In ballasted railway tracks, ballast fouling due to finer material intrusion has been identified as a challenging issue in track maintenance works. In this research, deformation characteristics of crushed stone-sand mixtures, simulating fresh and fouled ballasts were studied from laboratory and a 3-D discrete element method (DEM) triaxial compression tests. The DEM simulation was performed using a recently developed DEM approach, named, Yet Another Dynamic Engine (YADE). First, void ratio characteristics of crushed stone-sand mixtures were studied. Then, triaxial compression tests were conducted on specimens with 80 and 50% of relative densities simulating dense and loose states respectively. Initial DEM simulations were conducted using sphere particles. As stress-strain behaviour of crushed stone-sand mixtures evaluated by sphere particles were different from laboratory specimens, in next DEM simulations, the particles were modeled by a clump particle. The clump shape was selected using shape indexes of the actual particles evaluated by an image analysis. It was observed that the packing behaviour of laboratory crushed stone-sand mixtures were matched well with the DEM simulation with clump particles. The results also showed that the strength properties of crushed stone deteriorate when they are mixed by 30% or more of sand, specially under dense state. The results also showed that clump particles give closer stress-strain behaviour to laboratory specimens than sphere particles.

Keywords: discrete element method; fouled ballast; railway track; stress-strain behaviour; triaxial test

1. Introduction

In ballasted railway tracks, finer materials intrude and mix with fresh ballast, which is called ballast fouling, mainly due to repeated heavy train loads. The finer materials come either from the underneath layers (i.e., subballast and subgrade) and also due to particle crushing within ballast layer itself (Selig and Waters 1994, Indraratna *et al*. 2004, Hossain *et al*. 2007, Thakur *et al*. 2010). When the degree of ballast fouling is significant, a maintenance method needs to be applied to bring the settled sleepers into the original position. Due to huge costs and interruption to regular traffic, the ballast fouling has been identified as a main issue in track maintenance of the ballasted

*Corresponding author, Postdoctoral Fellow, Ph.D., E-mail: janaka_eng@yahoo.com
[a] Professor, Ph.D., E-mail: hayano@ynu.ac.jp

http://www.techno-press.org/?journal=gae&subpage=7 ISSN: 2005-307X (Print), 2092-6219 (Online)

railway tracks. Although concrete railway tracks bring less settlement, still ballasted railway tracks are preferred in the world due to their simplicity in the design and maintenance (Profillidis 2000).

The change in gradation curve of ballast, which is the immediate result from finer material intrusion, will result in different deformation characteristics in ballasted railway tracks. It has been reported that ballast fouling affects settlement behaviours in ballasted railway tracks (Indraratna *et al*. 2006, Huang and Tutumluer 2011, Kumara and Hayano 2013). While deformation characteristics of fresh ballast had been studied quite well in the past (Indraratna *et al*. 1998, Lackenby *et al*. 2007, Sevi1 and Ge 2012), only a very few studies had been conducted to study stress-strain behaviour of fouled ballast (Indraratna *et al*. 2011a, Rujikiatkamjorn *et al*. 2012). Although discrete element method (DEM) has been used quite widely in other engineering applications, it has not been fully utilised in understanding stress-strain behaviour of railway ballast, partly due to difficulties in simulating angular shape of ballast particles. In recent times, a few researchers adopted some DEM approaches in studying deformation characteristics of railway ballasts (Lobo-Guerrero and Vallejo 2006, Huang and Tutumluer 2011).

It is very important to understand effects of ballast fouling on the deformation characteristics of ballast to propose an effective maintenance plan for ballasted railway tracks. After development of DEM (Cundall 1971, Cundall and Strack 1979), DEM simulations became the most widely used numerical method to study deformation characteristics of granular materials. In this research, the deformation characteristics of crushed stone-sand mixtures, simulating fouled ballast were studied using triaxial compression tests in the YADE, a recently developed open source code (Smilauer *et al*. 2010). The results from DEM simulations were compared with those of laboratory triaxial compression tests.

1.1 YADE

YADE is an extensible open-source framework for discrete numerical models, focused on discrete element method (Kozicki and Donze 2008). In this research, the available code (written in C++) was modified to obtain gap-graded gradation curves in simulating crushed stone-sand mixtures. The available original code can be used to simulate only uniform-nature gradation curves (e.g., observed in fresh ballast) (Widulinski *et al*. 2009, Kumara *et al*. 2012b, Kumara 2013). In this research, initially, crushed stone and sand were simulated by sphere particles. In next part of DEM simulations, the particle was changed to a clump shape to simulate angular crushed stone accurately. It has also been reported that sphere particles give relatively smaller stress-strain behaviour than angular materials (Rothenburg and Bathurst 1992, Lin and Ng 1997, Szarf *et al*. 2011). In triaxial compression test simulation, the stress-strain behaviour was modelled by elastic-perfectly plastic constitutive model for crushed stone-sand mixtures. Recently, a few researchers used the YADE to conduct triaxial compression tests and found consistent results with the laboratory experiments (Scholtes *et al*. 2009, Widulinski *et al*. 2009, Dang and Meguid 2010). More details on the YADE can be found in Smilauer *et al*. (2010).

2. Methodology

2.1 Laboratory experiments

In ballasted railway tracks, generally, ballast is laid over sub-ballast up to 250 mm thickness (see Fig. 1). As ballast particles vary from 10-60 mm in the field, it is difficult to use same size

ballasts in laboratory testing apparatus unless large-scale testing apparatus are available. Therefore, in this research, crushed stone, approximately 1/5th size of the field ballast were used as fresh (or clean) ballast (see Fig. 2(a)). The field ballast and the crushed stone tested in the research are generally produced from the same source. At the crushing plants, large-sized particles (e.g., used as field ballast) and small-sized particles (e.g., used in concrete mixtures or similar sizes used in our experiments) are produced using different crushing rates. As reported by Marschi *et al*. (1972) and Indraratna *et al*. (1998), scaled-down particles may produce a slightly higher internal frictional angle, ϕ (e.g., a reduction of 2-3° of ϕ when the particle size is increased from 7-39 mm). However, as reported by Vallerga *et al*. (1957) and Indraratna and Salim (2005), the most importance factors of the ballast are the parent rock and the particle shapes. Recently, Pen *et al*. (2013) tested railway ballasts with different particle sizes varying from 9.5-62.5 mm to study the angularity of particles. As reported by Pen *et al*. (2013), due to a negligible variation in angularity, scaled-down materials are appropriate substitutes for testing purposes. Since we used crushed stone with similar angularities as railway ballast, we assume that the crushed stone simulates field ballast reasonably well.

Medium-size sand was used as fouling material (see Fig. 2(b)). Crushed stone-sand mixtures of different sand percentages were used as fouled ballast specimens. The same materials were used in a series of model tests to study settlement characteristics of fresh and fouled ballasts subjected to the tamping maintenance application (Kumara and Hayano 2013, Kumara *et al*. 2015). We did not

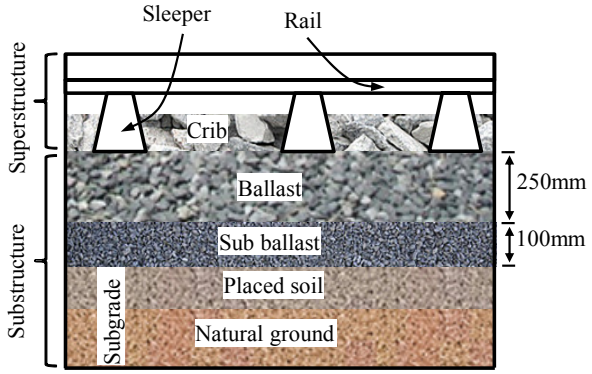

Fig. 1 Schematic figure of a ballasted railway track

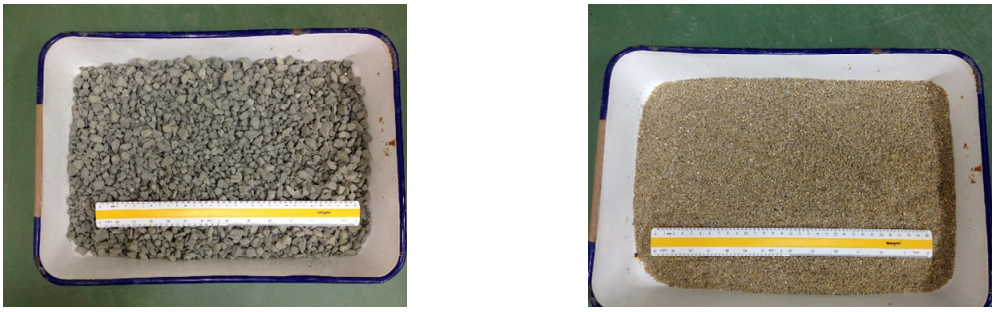

(a) (b)

Fig. 2 A photograph of (a) crushed stone; and (b) sand

include very small particles as fouling material since the particle image velocimetry (PIV) method adopted in the study cannot track particle movements when they are very small (e.g., the size of Toyoura sand). Also, fouling materials can be varied in nature depending on the source of them as reported by Selig and Waters (1994) and Indraratna *et al*. (2011b). Therefore, the fouled ballast tested in this study simulates the field conditions reasonably well.

The percentage of sand in the crushed stone-sand mixtures were varied. In addition to pure specimens of crushed stone and sand, four different crushed stone-sand specimens were selected with 15, 30, 50 and 70% of sand respectively. As fouled ballast with less than 10% of fouling materials is not significant for deformation characteristics, we selected crushed stone-sand specimens with 15% or more of sand (Selig 1985).

At the first step, void ratio characteristics of crushed stone-sand mixtures were studied using laboratory density tests (JIS 2009). Eqs. (1.1) and (1.2) give maximum and minimum void ratio, e_{max} and e_{min} respectively. In Eqs. (1.1) and (1.2), it is assumed a 1000 kg/m^3 for water density and 2.65 for specific gravity for crushed stone and sand. In the next step, the stress-strain behaviours of crushed stone-sand mixtures were evaluated by laboratory triaxial compression tests (JGS 1998). Triaxial compression tests were conducted using 100 mm diameter and 200 mm high specimens under both dense and loose states, prepared by 80 and 50% of relative density respectively. The steps of the sample preparation is shown in Fig. 3 where the required relative density was achieved by a pre-defined number of hits by a small hammer as shown in Fig. 3(b). Axial stress and axial deformation were measured by a load cell and an external displacement transducer respectively as shown in Fig. 4. The triaxial compression tests were conducted under 80 kPa of confining pressure, σ_c. Although ballast in a general railway tracks is subjected to 40-50 kPa of σ_c, the triaxial compression tests were conducted under 80 kPa to minimize errors arising from a small suction pressure (e.g., membrane force effects, etc.). Effects of confining pressure on the deformation characteristics of railway ballast can be found in Lackenby *et al*. (2007) and Thakur *et al*. (2012).

$$e_{max} = \frac{G_s \rho_w}{\rho_{d,min}} - 1 \tag{1.1}$$

Where e_{max} is maximum void ratio, G_s is specific gravity, ρ_w is water density and $\rho_{d,min}$ is minimum dry density

$$e_{min} = \frac{G_s \rho_w}{\rho_{d,max}} - 1 \tag{1.2}$$

Where e_{min} is minimum void ratio, G_s is specific gravity, ρ_w is water density and $\rho_{d,max}$ is maximum dry density.

2.2 Image analysis

In image analysis, particle shape characteristics can be evaluated using 2D images. In this research, we conducted an image analysis using ImageJ (Ferreira and Rasband 2011). Crushed stone and sand particles were analysed to obtain circularity (see Eq. (2)) and ratio of minor and major axis (i.e., axis ratio) of the particles. Manually arranged particles on a black sheet were captured from the top using a Nikon D7000 camera. In ImageJ, once images are converted into binary version, different shape indexes (e.g., area, major axis, minor axis, circularity, etc.) can be obtained. In the image analysis, we applied some image processing techniques such as “Erode”,

(a) (b) (c)

Fig. 3 (a) Pouring materials into the mould; (b) tamping the mould by a hammer; and (c) a prepared specimen

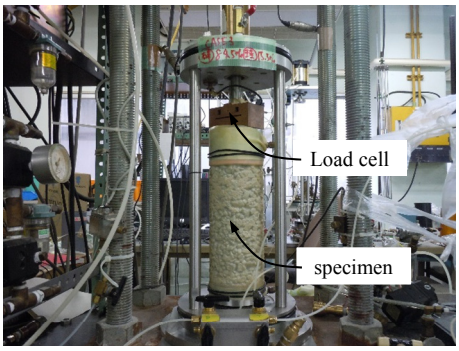

Fig. 4 A photograph of the triaxial apparatus

"Dilate" and "Fill Holes" to obtain quality images after converting original images into binary version. More details on "erode" and "dilation" processes can be found in Masad *et al*. (2001) and Al-Rousan *et al*. (2007). In the image analysis, both crushed stone and sand particles were assumed to be ellipse shape as that gives the closest shape to the actual shape among the shapes available in ImageJ. More details on the image analysis process can be found in Kumara *et al*. (2012a, c).

$$C = \frac{4\pi \times A}{P^2} \tag{2}$$

Where C is circularity, A is area and P is perimeter of an ellipse particle.

2.3 DEM simulation

In DEM simulation of triaxial compression test, the void ratio is controlled by friction angle during isotropic compression, ϕ_{iso}. First, the maximum and minimum void ratios, e_{max} and e_{min} respectively were determined assigning values from 0° until void ratio does not increase with the friction angle. Then, the void ratios related to 80 and 50% of relative densities, e_{80} and e_{50} respectively, were obtained by adjusting ϕ_{iso} as given in Table 1. The friction angle in isotropic compression for 80 and 50% of relative densities, $\phi_{iso,80}$ and $\phi_{iso,50}$ respectively, were obtained by "trial and error" method by adjusting ϕ_{iso}. In the DEM simulation, e_{max} and e_{min} were obtained by assigning 0° and 90° to ϕ_{iso} (Kumara *et al*. 2012b). In DEM simulation, the void ratio increases with ϕ_{iso}. While the minimum value of void ratio is observed with 0° of ϕ_{iso}, the maximum value is

almost reached with 90°. After 90° of ϕ_{iso}, void ratio remains constant with ϕ_{iso}. The input parameters used in the DEM simulation are given in Tables 1 and 2. In the DEM simulation, particle size was simulated as 100 times larger than the actual size to reduce simulation time. In general, larger particle size is used to reduce the simulation time (Belheine *et al*. 2009, Jiang *et al*. 2011). Although image analyses gave slightly different values of circularity and axis ratio, *C* and

Table 1 The input parameters of DEM simulations

Parameter	Value
Friction angle of particles in isotropic compression, ϕ_{iso}	See Table 2
Density of particles, ρ (kg/m^3)	2700
Number of clump particles, N	2500
Confining pressure, σ_c (kPa)	80
Friction angle of particles in shearing, ϕ_{shr}	See Table 2
Shear stiffness of particles, E (MPa)	See Table 2
Ratio of shear stiffness to normal stiffness	0.5
Strain rate (s^{-1})	0.03
Maximum velocity of walls, V_w (m/s)	0.1

Note: N is 10000 for sphere particle simulation

Table 2 The details of friction angles and stiffness

Percentage of sand, P_s (%)	Friction angle in isotropic compression (clump particles), ϕ_{iso} (degree)		Friction angle in shearing, ϕ_{shr} (degree)	Shear stiffness, E (MPa)
	D_r = 50%	D_r = 80%		
0	17.5	5.0	45.0	150
15	14.0	5.0	42.8	130
30	13.5	4.5	40.5	110
50	12.0	4.5	37.5	82
70	18.0	8.7	34.5	56
100	21.0	6.0	30.0	15

Note: ϕ_{iso} were slightly different for sphere particles and D_r is relative density

(a) (b)

Fig. 5 (a) The clump particle; and (b) cross-sectional view of it

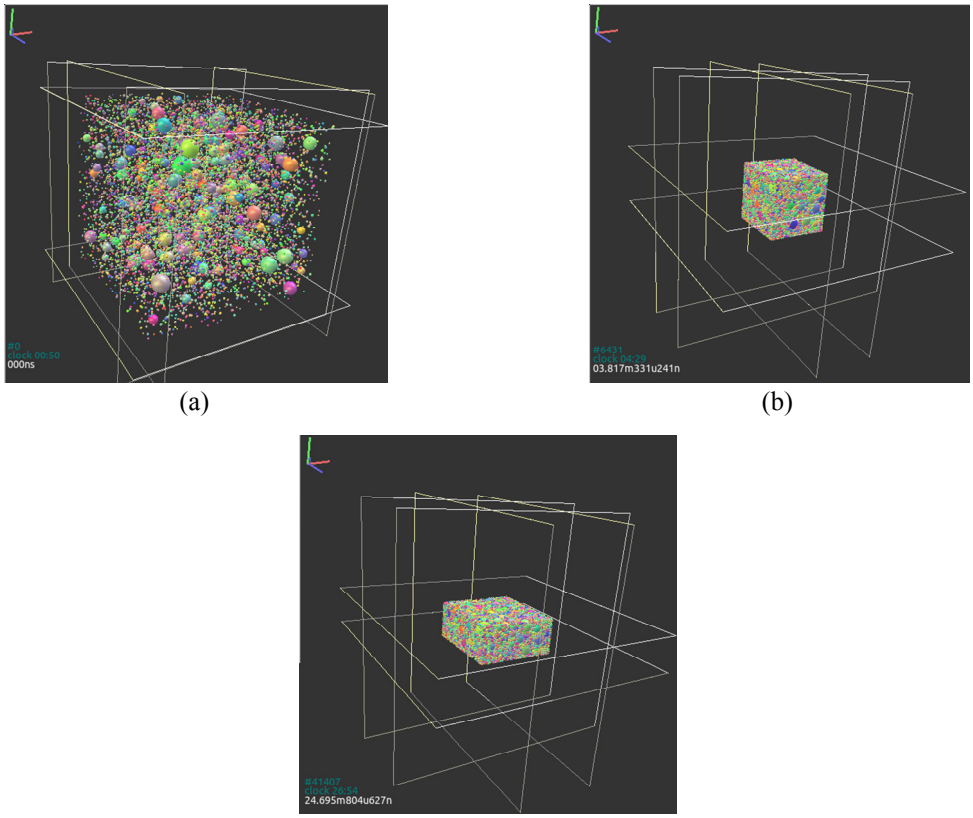

(a) (b) (c)

Fig. 6 A DEM simulation (a) at sample generation; (b) after isotropic compression; and (c) after shearing

b/*a* respectively (*a* and *b* are major and minor axis of an ellipse respectively) for crushed stone and sand particles, both crushed stone and sand particles were simulated using the same clump shape shown in Fig. 5. The clump shape is a combination of 4 equal-size spheres (McDowell *et al*. 2011). In DEM simulation, the specimen was prepared in a cubic shape box where the boundaries are constructed by rigid walls. The loading is applied by moving the top and bottom walls by applying a velocity to the walls as given in Table 1. A similar method in conducting triaxial compression test in the YADE had been reported in Scholtes *et al*. (2009) and Widulinski *et al*. (2009). However, in their simulations, only sphere particles were used. Fig. 6 shows a simulation of triaxial compression test at different steps using a crushed stone-sand specimen. As shown in Fig. 6(a), at the beginning of particle generation, the packing is very loose. At the end of isotropic compression (see Fig. 6(b)), the void ratio was obtained to compare with laboratory specimens.

3. Results and discussion

3.1 Image analysis results

The results of image analysis on crushed stone and sand particles are given in Table 3. It also gives the results of circularity and axis ratio, *C* and *b*/*a* respectively for a sphere and the clump

Table 3 The results of image analysis

Material	Circularity, C	Axis ratio, b/a
Crushed stone	0.704	0.721
Sand	0.866	0.778
Sphere	1.000	1.000
Clump	0.819	0.826

particle. As given in Table 3, sand is more rounded than crushed stone. However, due to difficulty in simulating the exact shape, we simulated both crushed stone and sand particles by the same clump particle which simulate the field ballast and fouling material better than sphere particles.

3.2 Void ratio characteristics

Fig. 7 shows particle size distribution of laboratory and DEM-simulated specimens. As shown in Fig. 7(c), the crushed stone-sand specimen with 70% of sand is not smooth as laboratory

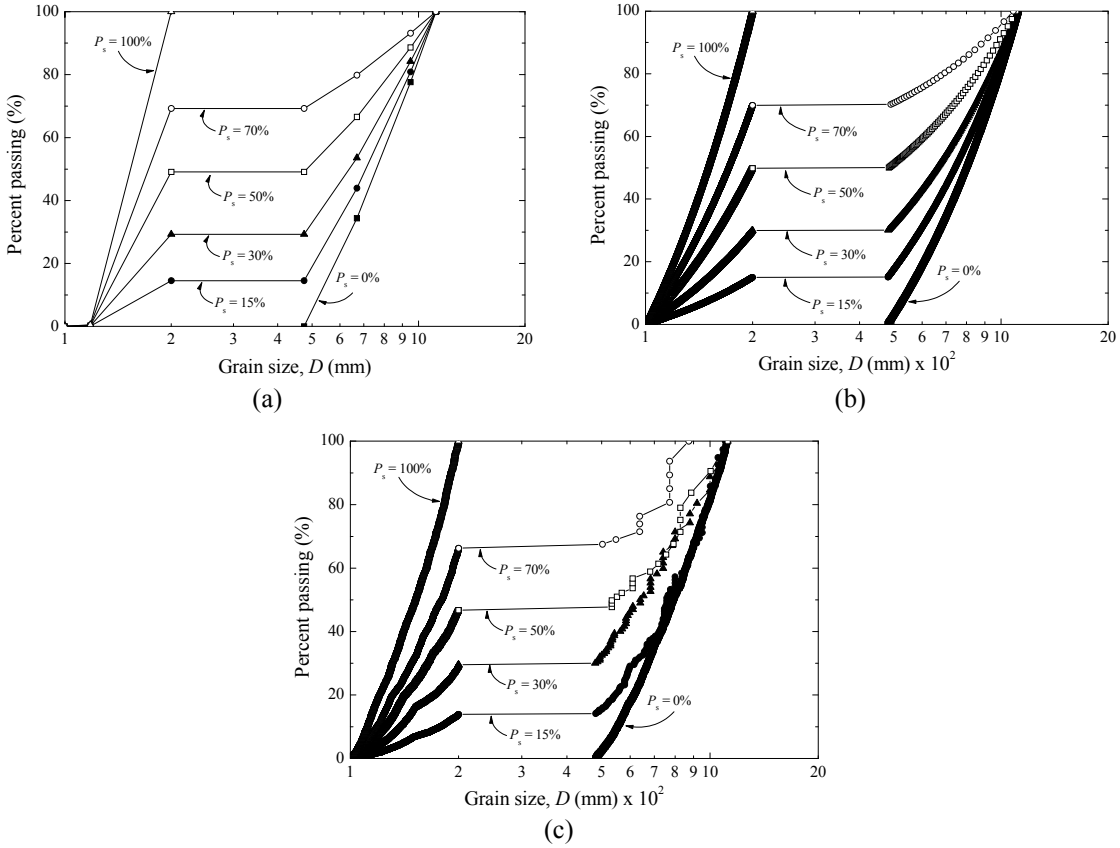

Fig. 7 Particle size distribution of (a) laboratory specimens; (b) DEM simulations with sphere; and (c) clump particles (P_s is percentage of sand)

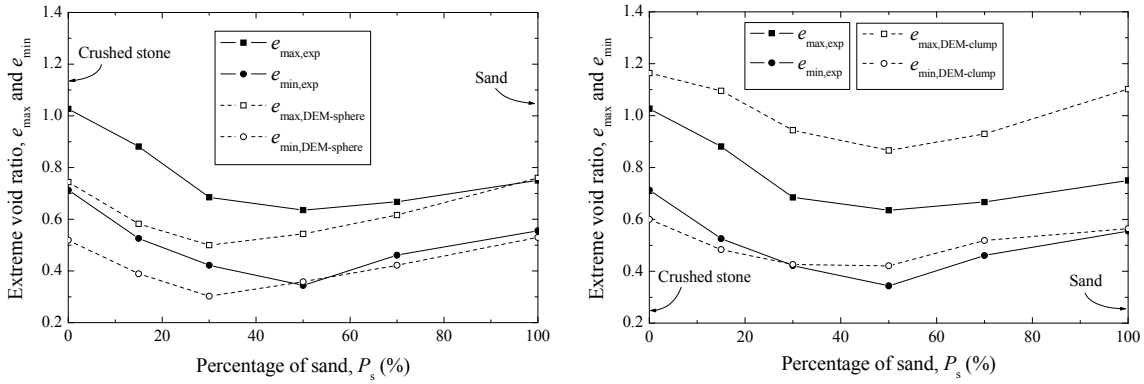

Fig. 8 The comparisons of extreme void ratios between laboratory specimens and DEM simulations with (a) sphere; and (b) clump particles

specimen or the DEM simulation with sphere particles, probably, due to less number of larger particles (i.e., crushed stone). However, in other cases, the gradation curves of DEM simulations are same as the laboratory specimens. Fig. 8 shows a comparison of the extreme void ratio (e_{max} and e_{min}) variations with percentage of sand among the three methods (i.e., laboratory specimens and DEM simulations with sphere and clump particles). In Fig. 8, $e_{max,exp}$ and $e_{min,exp}$ are respective void ratios from laboratory experiments, $e_{max,DEM\text{-}sphere}$ and $e_{min,DEM\text{-}sphere}$ are respective void ratios from DEM simulation with sphere particles, and $e_{max,DEM\text{-}clump}$ and $e_{min,DEM\text{-}clump}$ are respective void ratios from DEM simulation with clump particles. As shown in Fig. 8(a), void ratios decreased with percentage of sand, P_s up to the specimen with 50% of sand in laboratory specimens. After making the densest packing with 50% of sand, void ratios increased with percentage of sand up to sand (i.e., P_s = 100%). In DEM simulations with sphere particles, void ratios decreased with P_s up to the specimen with 30% of sand. After making the densest packing with 30% of sand, void ratios increased with P_s up to sand (i.e., P_s = 100%). The difference in percentage of sand to reach minimum values of void ratios (i.e., the densest packing) might be attributed to the difference in particle shape as DEM simulations were conducted using sphere particles whereas laboratory specimens consist of irregular shape particles. However, in Fig. 8(b) when clump particles were used in DEM simulations, void ratios decreased with P_s and produced the densest packing with 50% of sand before increasing with P_s up to the sand same as the laboratory specimens. A few researchers, including Lade *et al*. (1998) and Cubrinovski and Ishihara (2002) also reported similar results on void ratio characteristics of binary mixtures where variations of void ratio of binary mixtures with percentage of finer material were discussed. The results show that angular shape clump particles simulate the packing behaviour of crushed stone and sand better than round shape sphere particles. However, it should be noted that e_{max} is higher than sphere particles, perhaps, the assigned 90° for ϕ_{iso} may give looser state compared to laboratory specimens. Since the minimum value of e_{min} is obtained by assigning 0° for ϕ_{iso} (which is the possible minimum value), the results of e_{min} are same as the laboratory specimens.

3.3 Triaxial test results

Fig. 9 shows stress-strain behaviour of crushed stone-sand mixtures for dense and loose states

from laboratory experiments. The results clearly show that crushed stone has higher strength properties than sand both under dense and loose states. As expected, the specimens with 80% of relative density (i.e., dense specimens) show higher strength properties in both laboratory specimens and DEM simulations. Salot *et al*. (2009) also reported similar findings on DEM simulations. Crushed stone does not show clear failure plane (i.e., peak deviator stress) even after significant post-peak straining (e.g., 15%) both under dense and loose states. In loose state, all the specimens apart from the ones closer to the densest specimen (i.e., with 30 and 50% of sand), show strain hardening behaviour. In dense state, all the specimens apart from the specimens of less than 15% of sand show strain softening behavior as could be seen in fresh and moderately fouled ballasts. The results suggest that stress-strain behaviour of crushed stone-sand mixtures are affected by relative density in addition to percentage of sand. Figs. 10 and 11 show stress-strain behaviour of crushed stone-sand specimens from DEM simulations with sphere and clump particles respectively. The results clearly show that deviator stress (at same strain levels) of sphere particles is much smaller than the laboratory specimens. However, deviator stress increased in the

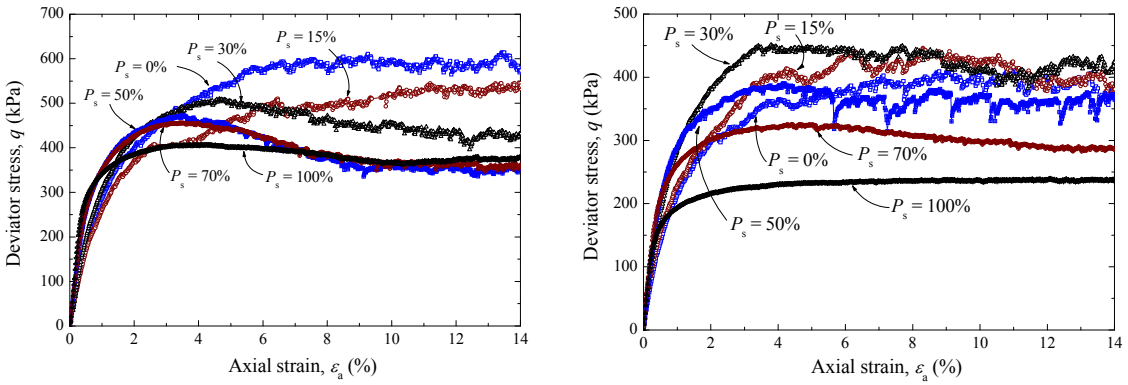

Fig. 9 Stress-strain behaviours of laboratory specimens under (a) dense; and (b) loose states (P_s is percentage of sand)

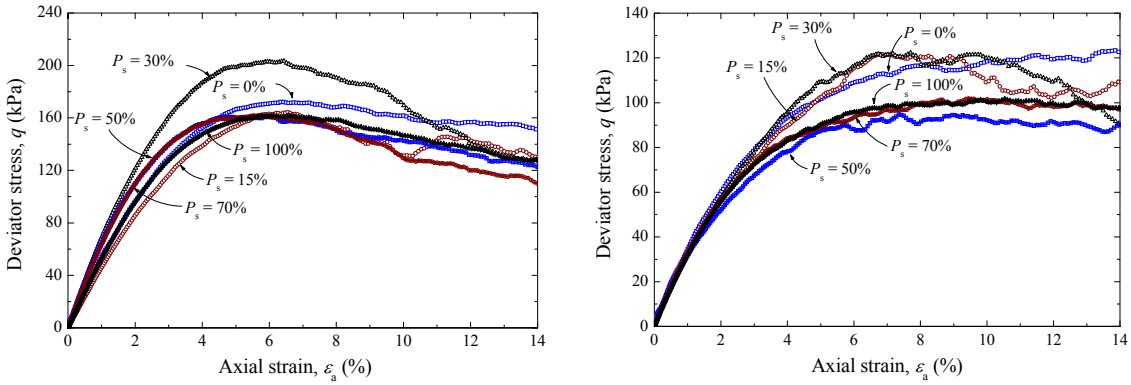

Fig. 10 Stress-strain behaviours of DEM simulations with sphere particles under (a) dense; and (b) loose states (P_s is percentage of sand)

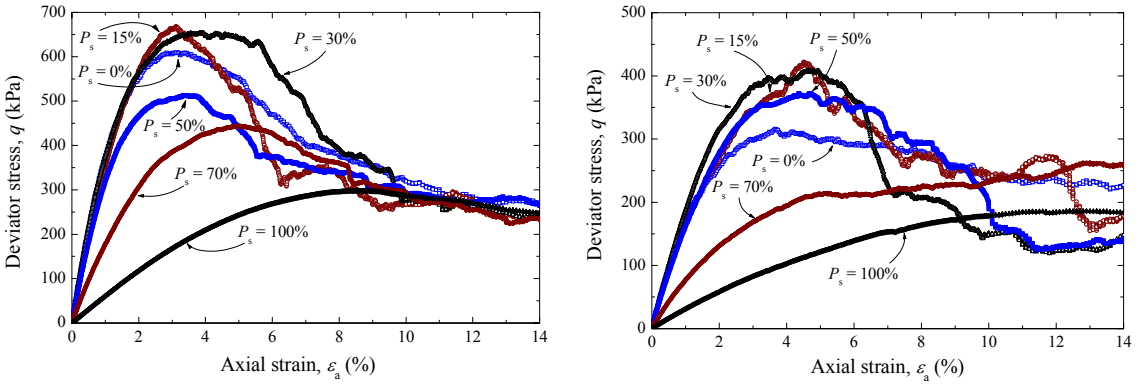

Fig. 11 Stress-strain behaviours of DEM simulations with clump particles under (a) dense; and (b) loose states (P_s is percentage of sand)

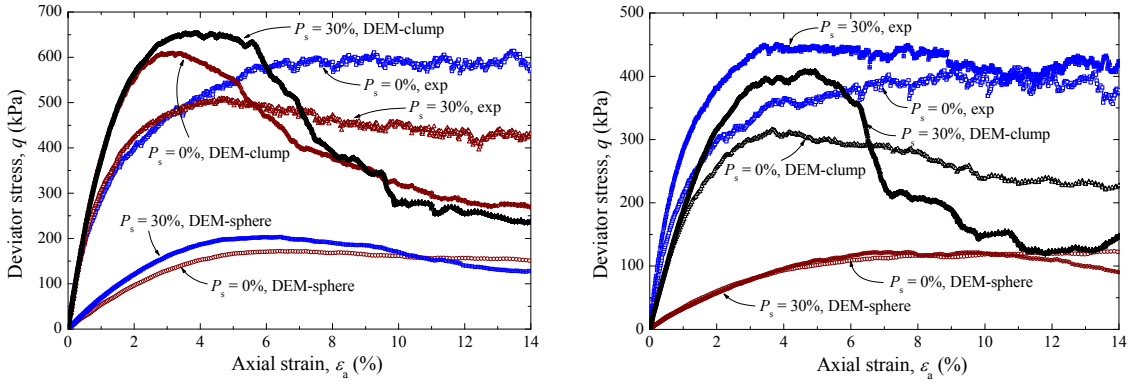

Fig. 12 The comparisons of stress-strain behaviours among three methods under (a) dense; and (b) loose states (P_s is percentage of sand)

DEM simulations with clump particles and has similar values to the laboratory specimens. As shown in Figs. 10 and 11, in DEM simulations too, the specimens closer to its parent material show strain hardening while crushed stone-sand specimens closer to the densest packing show strain softening behaviour. Also, the looser specimens show more strain hardening behaviour than denser specimens same as the laboratory specimens. Fig. 12 shows comparisons of stress-strain behaviour among the three methods (i.e., laboratory specimens, DEM simulations with sphere and clump particles) for pure materials of crushed stone and sand, and the crushed stone-sand mixture of 30% of sand. The results clearly suggest that sphere particle is not good to simulate stress-strain behaviour of crushed stone or crushed stone-sand mixtures as they show relatively lower deviator stress. It also shows that clump particles is closer to crushed stone as exhibiting similar stress-strain behaviours as the laboratory specimens.

Mohr-Coulomb failure criteria can be written as in Eq. (3.1). Eq. (3.1) can be rewritten as Eq. (3.2) for dry sand at the failure. Eq. (3.2) can be written in a simple way as in Eq. (3.3) using deviator stress and mean stress. Since a clear failure point is not obtained for many specimens (i.e.,

in strain hardening cases), the respective peak stresses were taken as the failure stresses. Therefore, the peak frictional angle can be obtained as given in Eq. (4). Fig. 13 shows a comparison of the peak friction angle versus dry density between laboratory specimens and DEM specimens. As shown in Fig. 13, under both dense and loose states, the peak friction angle reduces with the percentage of sand beyond 30% of sand. Therefore, we can say that the strength properties of crushed stone deteriorate after mixing with 30% or more of sand under both dense and loose states. Indraratna *et al*. (1998) also has reported similar peak friction angles for fresh ballast. The variation of the peak frictional angle with relative density in the laboratory specimens are matched better by DEM simulations with clump particles, particularly due to similar peak frictional angles than spherical particles. Due to lesser angularity of sphere particles compared to clump particles, they produced relatively smaller peak friction angles under both dense and loose states. We can clearly see here that clump particles simulate crushed stone and sand particles better than sphere particles. However, a much similar particle shape (i.e., more angular shape) in the DEM simulation would result in exact behaviour as the laboratory specimens.

$$\sin\phi' = \frac{\left(\sigma'_a - \sigma'_c\right)/2}{c'\cot\phi' + \left(\sigma'_a + \sigma'_c\right)/2} \tag{3.1}$$

Where σ_a, σ_c are axial and confining stress at the failure respectively, c is cohesion and ϕ is friction angle.

$$\sin\phi_f = \frac{\left(\sigma_{af} - \sigma_{cf}\right)/2}{\left(\sigma_{af} + \sigma_{cf}\right)/2} \tag{3.2}$$

Where σ_{af}, σ_{cf} are axial and confining stress respectively, and ϕ_f is frictional angle at the failure.

$$\sin\phi_f = \frac{q_f}{p_f} \tag{3.3}$$

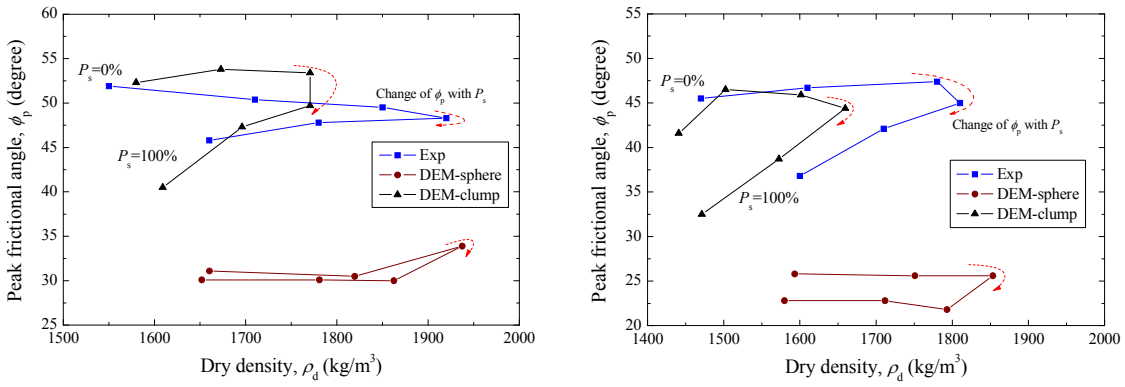

Fig. 13 The comparisons of peak frictional angle versus dry density among the three methods for (a) dense; and (b) loose state (P_s is percentage of sand)

Where q_f and p_f are deviator stress and mean stress respectively at the failure.

$$\sin\phi_p = \frac{q_p}{p_p} \tag{4}$$

Where q_p and p_p are peak deviator stress and mean stress respectively.

4. Conclusions

In this study, triaxial compression tests on crushed stone-sand specimens simulating fouled ballast were conducted using a recently developed discrete element method (DEM), named YADE. The triaxial compression tests were conducted for dense and loose specimens with 80 and 50% of relative densities respectively. The initial DEM simulations were conducted using sphere particles, the default shape available in the YADE. However, as field ballast is angular in shape, the DEM simulations were then extended using a clump particle. The clump shape was proposed using the results of an image analysis conducted on crushed stone and sand particles. The following conclusions were drawn from this research.

- In laboratory specimens, the extreme void ratios, e_{max} and e_{min} (e_{max} and e_{min} are maximum and minimum void ratio respectively) decrease with percentage of sand, P_s up to 50% and then increase with it. In DEM simulations with sphere particles, both e_{max} and e_{min} decrease with P_s up to 30%. However, in DEM simulations with clump particles, both e_{max} and e_{min} decrease with P_s up to 50% same as the laboratory specimens, which suggests that the clump particles simulate the packing behaviour of crushed stone-sand mixtures closely than sphere particles.
- In all cases (i.e., laboratory tests and DEM simulations), effects of sand intrusions on stress-strain behaviours of crushed stone-sand mixtures were observed. While most of the specimens in loose state showed strain hardening behaviour, most specimens in dense state showed strain softening behaviour.
- In the methods (i.e., laboratory tests and DEM simulations), denser packing (i.e., crushed stone-sand mixture with 30-50% of sand) showed strain softening behaviour, particularly in dense state.
- Although there was difference in stress-strain behaviours between laboratory specimens and DEM simulations with sphere particles, the DEM simulations with clump particles give similar stress-strain behaviours as the laboratory specimens.
- The strength properties of crushed stone deteriorate after they mix with 30% or more of sand under both dense and loose states.

Acknowledgments

Japanese Government is acknowledged for the financial assistance provided to the first author through a Monbukagakusho scholarship to study in his PhD at Yokohama National University, Japan. Mr. Y. Shigekuni and Mr. K. Sasaki, former graduate students at Yokohama National University are also appreciated for their contributions during the research works. The first author also acknowledges the President and Prof. Yoshiaki Kikuchi of Tokyo University of Science

(TUS), Japan for the President Postdoctoral Fellowship offered to him to work at the TUS where this manuscript was prepared.

References

Al-Rousan, T., Masad, E., Tutumluer, E. and Pan, T. (2007), "Evaluation of image analysis techniques for quantifying aggregate shape characteristics", *Construct. Build. Mater.*, **21**(5), 978-990.

Belheine, N., Plassiard, J.-P., Donze, F,-V., Darve, F. and Seridi, A. (2009), "Numerical simulation of drained triaxial test using 3D discrete element modeling", *Comput. Geotech.*, **36**(1-2), 320-331.

Cubrinovski, M. and Ishihara, K. (2002), "Maximum and minimum void ratio characteristics of sands", *Soil. Found.*, **42**(6), 65-78.

Cundall, P.A. (1971), "A computer model for simulating progressive, large scale movements in blocky rock systems", *Proceedings of Symposium of International Society of Rock Mechanics*, Nancy, France, September.

Cundall, P.A. and Strack, O.D.L. (1979), "A discrete numerical model for granular assemblies", *Geotechnique*, **29**(1), 47-65.

Dang, H.K. and Meguid, M.A. (2010), "Algorithm to generate a discrete element specimen with predefined properties", *Int. J. Geomech.*, **10**(2), 85-91.

Ferreira, T. and Rasband, W. (2011), *The Image J User Guide 1.44*.

Hossain, Z., Indraratna, B., Darve, F. and Thakur, P.K. (2007), "DEM analysis of angular ballast breakage under cyclic loading", *Geomech. Geoeng.*, **2**(3), 175-181.

Huang, H. and Tutumluer, E. (2011), "Discrete element modeling for fouled railroad ballast", *Construct. Build. Mater.*, **25**(8), 3306-3312.

Indraratna, B. and Salim, W. (2005), *Mechanics of Ballasted Rail Tracks – A Geotechnical Perspective*, Taylor and Francis, London, UK.

Indraratna, B., Ionescu, D. and Christie, H.D. (1998), "Shear behaviour of railway ballast based on large scale triaxial testing", *J. Geotech. Geoenviron. Eng.*, **124**(5), 439-449.

Indraratna, B., Shahin, M., Rujikiatkamjorn, C. and Christie, D. (2004), "Stabilisation of ballasted rail tracks and underlying soft formation soils with geosynthetics grids and drains", *Proceedings of GeoShanghai International Conference*, Shanghai, China, June.

Indraratna, B., Khabbaz, H., Salim, W. and Christie, D. (2006), "Geotechnical properties of ballast and the role of geosynthetics in rail track stabilisation", *Ground Improve.*, **10**(3), 91-101.

Indraratna, B., Ngo, N.T. and Rujikiatkamjorn, C. (2011a), "Behavior of geogrid-reinforced ballast under various levels of fouling", *Geotext. Geomembr.*, **29**(3), 313-322.

Indraratna, B., Su, L. and Rujikiatkamjorn, C. (2011b), "A new parameter for classification and evaluation of railway ballast fouling", *Can. Geotech. J.*, **48**(2), 322-326.

JGS (1998), *Method for Triaxial Compression Test on Unsaturated Soils* (*JGS 0527*), Japanese Geotechnical Society, Tokyo, Japan.

Jiang, M.J., Yan, H.B., Zhu, H.H. and Utili, S. (2011), "Modeling shear behavior and strain localization in cemented sands by two-dimensional distinct element method analyses", *Comput. Geotech.*, **38**(1), 14-29.

JIS (2009), Test method for minimum and maximum densities of sands (JIS A 1224); Japanese Industrial Standards, Tokyo, Japan.

Kozicki, J. and Donze, F.V. (2008), "A new open-source software developed for numerical simulations using discrete modeling methods", *Comput. Method. Appl. Mech. Eng.*, **197**(49-50), 4429-4443.

Kumara, G.H.A.J.J. (2013), "Development of prediction methods for deformation characteristics of fouled ballasts based on laboratory experiments and discrete element method", Ph.D. Dissertation; Yokohama National University, Yokohama, Japan.

Kumara, J. and Hayano, K. (2013), "Model tests on settlement behaviour of ballasts subjected to sand intrusion and tie tamping application", *Proceedings of 18th International Conference on Soil Mechanics and Geotechnical Engineering*, Paris, France, September.

Kumara, G.H.A.J.J., Hayano, K. and Ogiwara, K. (2012a), "Image analysis techniques on evaluation of particle size distribution of gravel", *Int. J. GEOMATE*, **3**(1), 290-297.
Kumara, G.H.A.J.J., Hayano, K., Sasaki, K. and Shigekuni, Y. (2012b), "Evaluation of void ratio characteristics of sand-gravel mixtures with different PSD curves by 3D DEM simulations", *Proceedings of 14th JSCE International Summer Symposium*, Nagoya, Japan, September.
Kumara, J.J., Ogiwara, K., Hoshi, S. and Hayano, K. (2012c), "Evaluation on grain size distribution of railway ballast with and without sands by image analyses", *Proceedings of 3rd International Conference on New Developments in Soil Mechanics and Geotechnical Engineering*, Nicosia, Turkey, June.
Kumara, J.J., Hayano, K. and Kikuchi, Y. (2015), "Study on settlement characteristics of fouled ballast for an effective maintenance method", *Proceedings of International Conference on Geotechnical Engineering*, Colombo, Sri Lanka, August.
Lackenby, J., Indraratna, B., McDowell, G. and Christie, D. (2007), "Effect of confining pressure on ballast degradation and deformation under cyclic triaxial loading", *Geotechnique*, **57**(6), 527-536.
Lade, P.V., Liggio, C.D. Jr. and Yamamuro, J.A. (1998), "Effects of non-plastic fines on minimum and maximum void ratios of sand", *Geotech. Test. J.*, **21**(4), 336-347.
Lin, X. and Ng, T.T. (1997), "A three-dimensional discrete element model using arrays of ellipsoids", *Geotechnique*, **47**(2), 319-329.
Lobo-Guerrero, S. and Vallejo, L.V. (2006), "Discrete element method analysis of railtrack ballast degradation during cyclic loading", *Granular Matter*, **8**(3-4), 195-204.
Marschi, N.D., Chan, C.K. and Seed, H.B. (1972), "Evaluation of properties of rockfill materials", *J. Soil Mech. Found. Div.*, **98**(1), 95-114.
Masad, E., Olcott, D., White, T. and Tashman, L. (2001), "Correlation of fine aggregate imaging shape indices with asphalt mixture performance", *Transportation Research Record: J. Transport. Res. Board*, **1757**, 148-156.
McDowell, G., Li, H. and Lowndes, I. (2011), "The importance of particle shape in discrete-element modelling of particle flow in a chute", *Geotech. Lett.*, **1**(3), 59-64.
Pen, L.M.L., Powrie, W., Zervos, A., Ahmed, S. and Aingaran, S. (2013), "Dependence of shape on particle size for a crushed rock railway ballast", *Granular Matter*, **15**(6), 849-961.
Profillidis, V.A. (2000), *Railway Engineering*, Ashgate Publishing Limited, Aldershot, UK.
Rothenburg, L. and Bathurst, R.J. (1992), "Micromechanical features of granular materials with planar elliptical particles", *Geotechnique*, **42**(1), 79-95.
Rujikiatkamjorn, C., Indraratna, B., Ngo, N.T. and Coop, M. (2012), "A laboratory study of railway ballast behaviour under various fouling degree", *Proceedings of 5th Asian Regional Conference on Geosynthetics*, Bangkok, Thailand, December.
Salot, C., Gotteland, P. and Villard, P. (2009), "Influence of relative density on granular materials behavior: DEM simulations of triaxial tests", *Granular Matter*, **11**(4), 221-236.
Scholtes, L., Chareyre, B., Nicot, F. and Darve, F. (2009), "Micromechanics of granular materials with capillary effects", *Int. J. Eng. Sci.*, **47**(1), 64-75.
Selig, E.T. (1985), "Ballast for heavy duty track", *Proceedings of Track Technology Conference*, Nottingham, UK, July.
Selig, E.T. and Waters, J.M. (1994), *Track Geotechnology and Substructure Management*, Thomas Telford, London, UK.
Sevil, A. and Ge, L. (2012), "Cyclic behaviors of railroad ballast within the parallel gradation scaling framework", *J. Mater. Civil Eng.*, **24**(7), 797-804.
Smilauer, V., Catalano, E., Chareyre, B., Dorofeenko, S., Duriez, J., Gladky, A., Kozicki, J., Modenese, C., Scholtes, L., Sibille, L., Stransky, J. and Thoeni, K. (2010), *Yade Reference Documentation*; Yade Documentation (V. Smilauer Ed.), The Yade Project (1st Ed.). (http://yade-dem.org/doc/)
Szarf, K., Combe, G. and Villard, P. (2011), "Polygons vs. clumps of discs: A numerical study of the influence of grain shape on the mechanical behaviour of granular materials", *Powder Technol.*, **208**(2), 279-288.
Thakur, P.K., Vinod, J.S. and Indraratna, B. (2010), "Effect of particle breakage on cyclic densification of

ballast: a DEM approach", *Proceedings of IOP Conference Series*: *Materials Science and Engineering*, Sydney, Australia, July.

Thakur, P.K., Vinod, B. and Indraratna, B. (2012), "Effect of confining pressure and frequency on the deformation of ballast", *Geotechnique*, **63**(9), 786-790.

Vallerga, B.A., Seed, H.B., Monismith, C.L. and Cooper, R.S. (1957), "Effect of shape, size and surface roughness of aggregate particles on the strength of granular materials", *ASTM Special Technical Publication*, **212**, 63-74.

Widlinski, L., Kozicki, J. and Tejchman, J. (2009), "Numerical simulations of triaxial test with sand using DEM", *Arch*. *Hydro-Eng*. *Environ*. *Eng*., **56**(3-4), 149-171.

CC